Spatial and temporal variations in plant Water Use Efficiency inferred from tree-ring, eddy covariance and atmospheric observations

Stefan C. Dekker[1*], Margriet Groenendijk[2*], Ben B. B. Booth[3], Chris Huntingford[4] and Peter M. Cox[2]

* Joint lead-authors

[1] *Copernicus Institute of Sustainable Development, Faculty of Geosciences, Utrecht University, Heidelberglaan 2, 3584 CS Utrecht, the Netherlands*

[2] *College of Engineering, Mathematics and Physical Sciences, University of Exeter, North Park Road, Exeter, EX4 4QF, UK*

[3] *Met Office Hadley Centre, FitzRoy Road, Exeter, EX1 3PB, UK*

[4] *Centre for Ecology and Hydrology, Benson Lane, Wallingford, OXON, OX10 8BB, UK*

Supporting Information

Section 1: Comparison to stomatal optimization theories

Katul et al (1) give the following expression for f (their Equation 15):

$$f = 1 - \sqrt{\frac{1.6\,\lambda D}{C_a}} \quad \text{(S1)}$$

where in general the Katul et al. theory assumes that λ depends on C_a. Substituting equation S1 into our Equation (2) for *WUE* gives the following expression:

$$WUE = \sqrt{\frac{\lambda\, C_a}{1.6\, D}} \quad \text{(S2)}$$

In the linear approximation to the Katul et al. theory, Palmroth et al. (2) state that λ is directly proportional to C_a, such that:

$$WUE = k\,\frac{C_a}{\sqrt{D}} \quad \text{(S3)}$$

where k is a constant.

Medlyn et al. (3) give the following expression for the *WUE* (their Equation 14):

$$WUE = \frac{C_a}{g_1\sqrt{D}+D} \quad \text{(S4)}$$

where g_1 is a constant. In general g_1 values are much larger than $\sqrt{D}$, so that:

$$WUE \approx \frac{C_a}{g_1\sqrt{D}} \quad \text{(S5)}$$

To derive effective a and b coefficients for each of these forms of *WUE* are calculated as:

$$a = \frac{\partial WUE}{\partial c_a}\frac{c_a}{WUE} \quad \text{(S6)}$$

$$b = \frac{\partial WUE}{\partial D}\frac{D}{WUE} \quad \text{(S7)}$$

from which we find that [a, b] = [1, -0.5] for both the models of Palmroth et al. (2) and Medlyn et al. (3).

Section 2: Partitioning the fractional change in humidity deficit a change in temperature and relative humidity

$$D = q_{sat}(1 - RH) \quad \text{(S8)}$$

$$\Delta D = \frac{\partial q_{sat}}{\partial T}(1 - RH)\Delta T - q_{sat}\Delta RH \quad \text{(S9)}$$

$$\frac{\Delta D}{D} = \frac{1}{q_{sat}}\frac{\partial q_{sat}}{\partial T}\Delta T - \frac{\Delta RH}{(1-RH)} \approx 0.07\Delta T - \frac{\Delta RH}{(1-RH)} \quad \text{(S10)}$$

Strictly ΔT in this equation is the surface (skin) temperature, but this is well approximated by the change in near surface air temperature, which is available from the global CRU dataset.

.

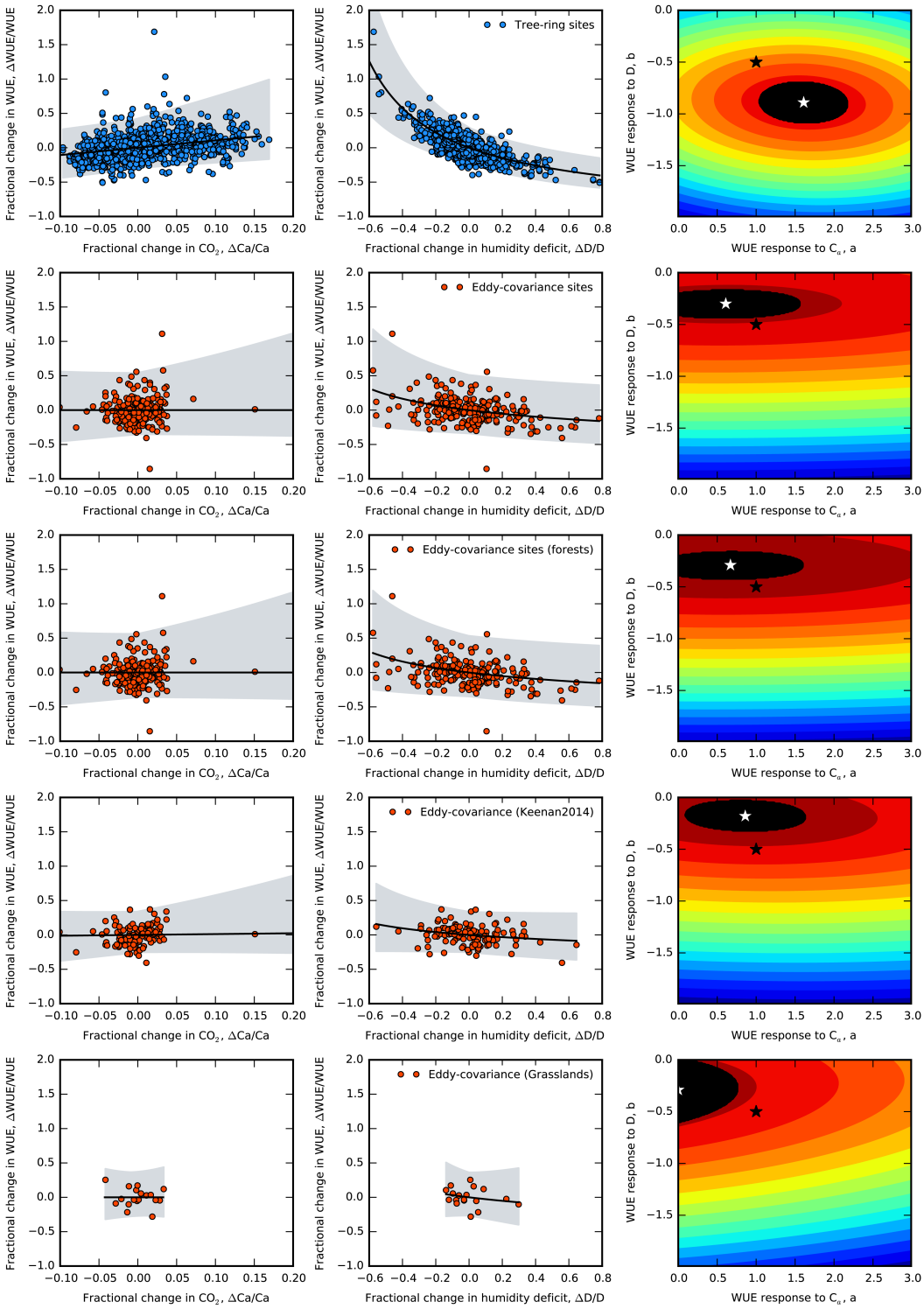

Fig. S1. Water Use Efficiency (*WUE*) from tree-ring and eddy-covariance observations as Fig. 1, but for different groups of sites. See also Table S3 for the values of *a* and *b* for each group.

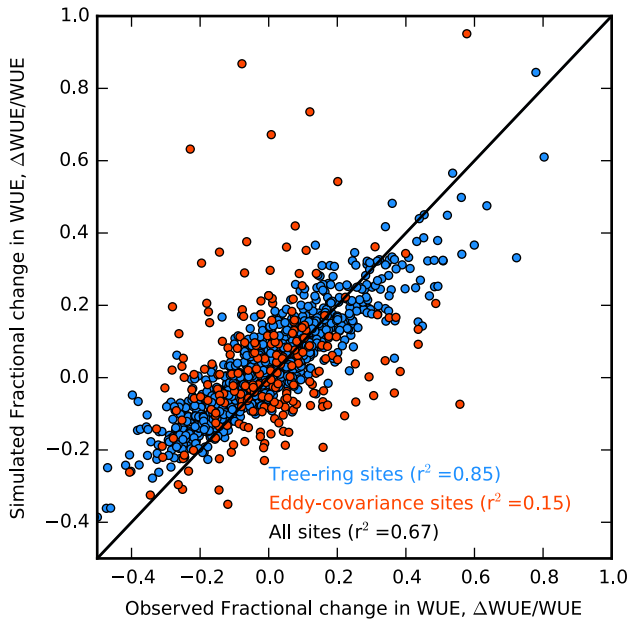

Fig. S2. Comparison of simulated and observed fractional change in *WUE* for the tree-ring and eddy-covariance sites.

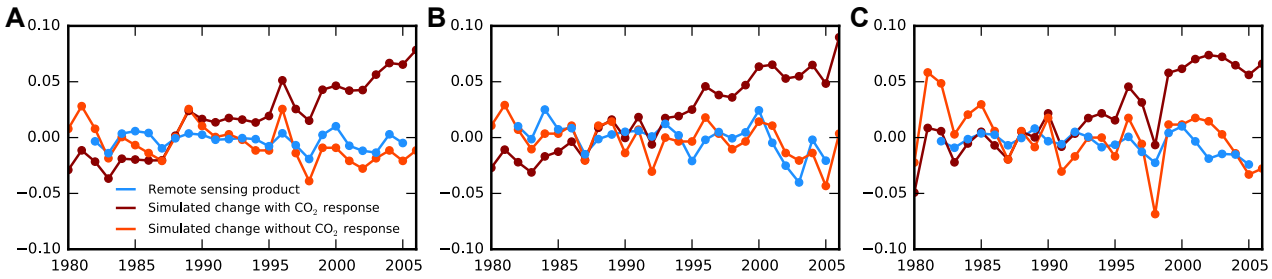

Fig. S3. Comparison of the (Andreu-Hayles et al., 2011; Arneth et al., 2002; Hemming et al., 1998) estimated fractional change in *WUE* with a remote sensing product for 3 different regions: (A) the Amazon, (B) South Africa and (C) South East Asia.

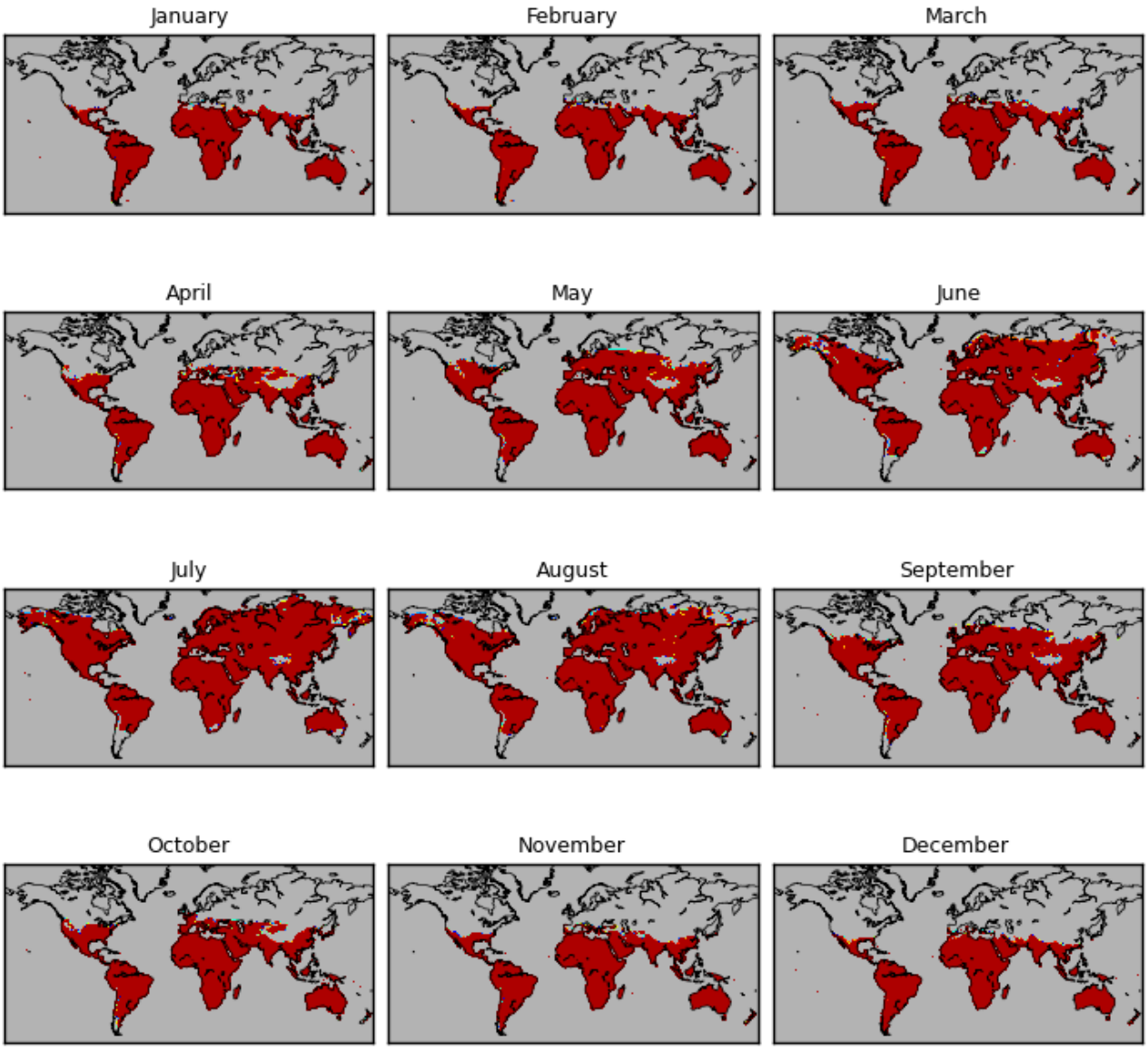

Fig S4. Monthly mask of the area included in the growing season. For each month the average temperature (1900-1930) from the CRU TS3.20 dataset was used to determine which areas were included in the growing season based on a 10°C threshold.

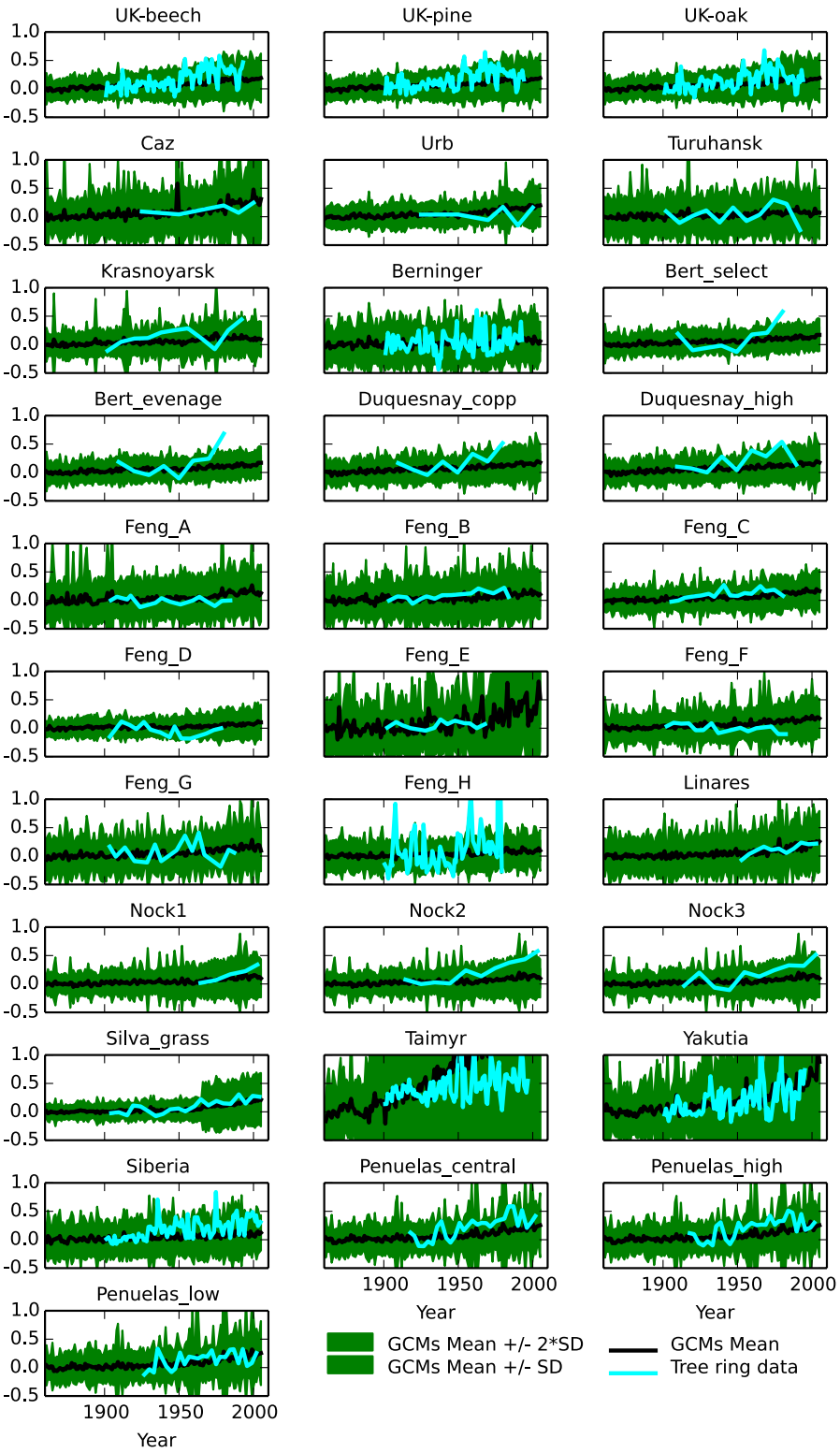

Fig. S5: Site by site comparisons of fractional WUE between the average regional ESMs climate projections and the tree ring data of the 31 site observations. Locations and details of the site observations can be found in table S2.

Table S1. Summary of the Fluxnet sites selected from the *Free Fair-use* dataset (www.fluxdata.org). The sites are selected based on data availability as described in the main text. *n* is the number of growing seasons with data available above the threshold of 10°C, *a* and *b* are the fitted parameter values from Equation (3) and r^2 is the coefficient of determination for this fit. Vegetation types are deciduous broadleaf forest (DBF), evergreen broadleaf forest (EBF), evergreen needleleaf forest (ENF), grassland (GRA), mixed forest (MF), wetland (WET) and woody savannah (WSA).

Site	Vegetation	Latitude	Longitude	$a \pm \sigma$	$b \pm \sigma$	*n*	r^2
AU-How	WSA	-12.49	131.15	-4.70±2.20	-2.86±1.25	6	0.63
BE-Bra	MF	51.31	4.52	-2.57±2.65	-0.76±0.23	6	0.77
BE-Vie	MF	50.31	6	0.01±0.51	-0.18±0.11	10	0.29
CZ-BK1	ENF	49.5	18.54	-10.27±6.80	-0.45±0.27	7	0.49
DE-Tha	ENF	50.96	13.57	0.68±1.79	-0.19±0.13	9	0.26
DK-Sor	DBF	55.49	11.65	0.81±0.69	0.34±0.40	10	0.20
ES-ES1	ENF	39.35	-0.32	1.24±0.74	-0.81±0.21	8	0.74
FI-Hyy	ENF	61.85	24.29	-0.25±1.47	-0.59±0.27	10	0.38
FI-Kaa	WET	69.14	27.3	4.38±5.52	-0.58±0.27	7	0.53
FR-Hes	DBF	48.67	7.06	1.69±2.56	-0.02±0.30	10	0.06
FR-LBr	ENF	44.72	-0.77	7.28±3.04	-0.10±0.25	8	0.51
FR-Pue	EBF	43.74	3.6	2.60±2.67	0.48±0.26	7	0.41
IL-Yat	ENF	31.35	35.05	-7.20±10.60	-1.00±1.29	6	0.16
IT-Col	DBF	41.85	13.59	-1.13±3.41	0.20±0.28	10	0.06
IT-Cpz	EBF	41.71	12.38	0.16±2.31	-0.48±0.13	8	0.79
IT-Ren	ENF	46.59	11.43	-10.39±4.30	0.12±0.26	8	0.65
IT-Ro1	DBF	42.41	11.93	4.00±5.59	-0.40±0.26	7	0.35
IT-SRo	ENF	43.73	10.28	7.90±1.53	-0.33±0.10	8	0.88
NL-Loo	ENF	52.17	5.74	-0.65±2.13	0.18±0.31	10	0.04
RU-Fyo	ENF	56.46	32.92	-0.45±1.89	-0.03±0.14	9	0.01
SE-Nor	ENF	60.09	17.48	-11.36±4.90	-0.84±0.30	6	0.75
UK-Gri	ENF	56.61	-3.8	-2.35±8.69	-1.10±0.94	6	0.42
US-Blo	ENF	38.9	-120.63	2.01±3.88	-1.21±0.82	10	0.29
US-Ha1	DBF	42.54	-72.17	2.81±3.07	0.46±0.26	7	0.46
US-Ho1	ENF	45.2	-68.74	3.88±1.87	0.10±0.17	9	0.38
US-Ton	WSA	38.43	-120.97	-3.42±3.58	-0.36±0.32	6	0.27
US-Var	GRA	38.41	-120.95	0.32±3.84	-0.28±0.67	6	0.05
US-WCr	DBF	45.81	-90.08	3.44±2.56	-0.44±0.21	8	0.49

Table S2. Summary of the tree-ring sites used in this study. *n* is the number of years with data available, *a* and *b* are the fitted parameter values from Equation (3) and r^2 is the coefficient of determination for this fit.

Site	Species	Lat	Lon	n	$a \pm \sigma$	$b \pm \sigma$	r^2	Reference
Woburn Abbey - beech	Fagus silvatica	52.23	-0.46	93	2.34±0.18	-0.71±0.06	0.86	Hemming et al. (1998)
Woburn Abbey - pine	Pinus sylvestris	52.23	-0.46	94	1.56±0.18	-0.73±0.06	0.79	Hemming et al. (1998)
Woburn Abbey - oak	Quercus robur	52.23	-0.46	94	1.76±0.17	-0.70±0.06	0.81	Hemming et al. (1998)
Caz	Pinus nigra	37.80	2.95	6	1.16±0.08	-1.08±0.09	0.98	Andreu-Hayles et al. (2011)
Urb	Pinus uncinata	42.23	1.70	6	0.78±0.38	-1.03±0.23	0.84	Andreu-Hayles et al. (2011)
Turuhansk	Pinus sylvestris	65.80	87.90	11	0.66±0.43	-1.40±0.25	0.79	Arneth et al. (2002)
Krasnoyarsk	Pinus sylvestris	56.00	92.90	11	1.71±0.33	-0.99±0.16	0.87	Arneth et al. (2002)
Berninger	Pinus sylvestris	68.46	25.93	74	0.84±0.12	-0.90±0.03	0.97	Berninger et al. (2000)
Bert_select	Abies alba	46.52	6.02	8	2.06±0.51	-0.94±0.15	0.98	Bert et al. (1997)
Bert_evenage	Abies alba	46.52	6.02	8	2.05±0.42	-1.02±0.13	0.98	Bert et al. (1997)
Duquesnay_copp	Fagus silvatica	49.00	6.00	8	0.92±0.44	-0.96±0.15	0.95	Duquesnay et al. (1998)
Duquesnay_high	Fagus silvatica	49.00	6.00	9	1.16±0.23	-0.90±0.09	0.97	Duquesnay et al. (1998)
Feng_A	Pinus edulis	37.43	-112.47	15	0.40±0.15	-0.86±0.11	0.84	Feng (1999)
Feng_B	Pinus edulis	37.50	-108.33	16	1.33±0.17	-0.91±0.17	0.83	Feng (1999)
Feng_C	Pinus longaeva	37.53	-118.22	16	0.93±0.14	-1.04±0.11	0.91	Feng (1999)
Feng_D	Fitzroya cupresoides	-40.05	-74.13	14	0.97±0.15	-0.92±0.05	0.98	Feng (1999)
Feng_E	Juniperous phoemicea	30.67	34.00	13	0.91±0.18	-0.89±0.10	0.88	Feng (1999)
Feng_F	Pinus ponderosa	35.92	-121.37	14	0.16±0.33	-0.68±0.17	0.74	Feng (1999)
Feng_G	Quercus lobata	34.15	118.73	15	0.54±0.31	-0.97±0.10	0.89	Feng (1999)
Feng_H	Picea sitchensis	57.92	-152.60	60	0.34±0.52	-0.94±0.06	0.98	Feng (1999)
Linares	Abies pinsapo	36.69	-5.02	11	1.35±0.09	-1.05±0.09	0.98	Linares et al. (2009)
Nock1	Melia	15.67	99.17	5	1.91±0.17	-0.45±0.24	0.99	Nock et al. (2011)
Nock2	Toona	15.67	99.17	10	2.22±0.18	-0.78±0.21	0.96	Nock et al. (2011)
Nock3	Chukrasia	15.67	99.17	10	2.02±0.19	-1.16±0.15	0.97	Nock et al. (2011)
Silva_grass	Araucaria angustifolia	-28.59	-48.82	21	1.12±0.09	-0.99±0.12	0.93	Silva et al. (2010)
Taimyr	Larix gmelinii	70.63	103.20	102	1.46±0.13	-1.00±0.05	0.86	Sidorova et al. (2010)
Yakutia	Larix gmelinii	70.00	148.00	78	2.48±0.31	-1.01±0.09	0.74	Sidorova et al. (2010)
Siberia	Larix gmelinii	64.53	100.23	102	1.82±0.05	-1.00±0.03	0.97	Sidorova et al. (2009)
Penuelas_central	Fagus sylvatica	41.77	2.43	29	2.29±0.19	-1.01±0.10	0.91	Penuelas et al. (2008)
Penuelas_high	Fagus sylvatica	41.77	2.43	29	1.77±0.18	-1.07±0.10	0.89	Penuelas et al. (2008)
Penuelas_low	Fagus sylvatica	41.77	2.43	25	0.94±0.15	-0.97±0.08	0.90	Penuelas et al. (2008)

Table S3. Comparison of *a* and *b* values from Equations 3 and 4 between tree-ring and eddy-covariance sites from Tables S2 and S3**.** The values of the combined datasets are compared to the values of the tree-ring or eddy-covariance sites only. The range is derived from the black areas in Fig. S2.

Description	***a***	***b***
Tree-rings + Eddy-covariance	1.51 ± 0.57	-0.72 ± 0.16
Tree-rings	1.61 ± 0.54	-0.89 ± 0.17
Eddy-covariance	0.79 ± 0.79	-0.30 ±0.10
Eddy-covariance (Keenan)	1.46 ± 0.78	-0.19 ± 0.10
Eddy-covariance (Forests)	0.90 ± 0.90	-0.29 ± 0.10
Eddy-covariance (Grasslands)	0.00 ± 0.00	-0.29 ± 0.29

Table S4. Comparison of the quality of the fits to observed *WUE* changes at *Fluxnet* sites, using varying numbers of environmental predictor variables. Our default model (equation 6) which uses just atmospheric CO_2 concentration (C_a) and atmospheric humidity deficit (D), is given by the first row of the table. The additional environmental predictors used are those readily available from a significant number (n) of *Fluxnet* sites: solar radiation at the surface (R_g), air temperature (T_a), and soil water content (*SWC*). The adjusted r^2 value accounts for the increase in the basic r^2 measure that is to be expected when additional parameters are introduced into a statistical model. Models with larger adjusted-r^2 values are therefore considered more robust, as they avoid over-fitting of the data.

Predictor Variables	***n***	***a***	***b***	r^2	***Adjusted*** r^2
C_a, D	227	1.028	-0.290	0.103	0.096
C_a, D, R_g	227	1.056	-0.309	0.105	0.093
C_a, D, R_g, T_a	227	1.124	-0.331	0.108	0.092
C_a, D, R_g, T_a, *SWC*	124	0.532	-0.416	0.118	0.081

Table S5. Fractional change in WUE simulated in the historical simulations of CMIP5 Earth System Models (ESMs). These are for research centres and models where both transpiration ("tran") and Gross Primary Productivity ("gpp") monthly variables are available, with ensemble size given in the 3rd column. The year 2005 normalised change (4th column) is relative to the mean over the modelled period from 1860 to 1890.

Research Centre	**Climate Model**	**Ensemble size**	**Fractional change in WUE by 2005**
BCC	bcc-csm1-1	3	0.19
BCC	bcc-csm1-1-m	1	0.21
BNU	BNU-ESM	1	0.20
CCCma	CanESM2	5	0.10
CMCC	CMCC-CESM	1	0.02
INM	inmcm4	1	0.07
IPSL	IPSL-CM5A-LR	6	0.15
IPSL	IPSL-CM5A-MR	3	0.14
IPSL	IPSL-CM5B-LR	1	0.16
MIROC	MIROC-ESM	3	0.03
MIROC	MIROC-ESM-CHEM	1	0.03
MPI-M	MPI-ESM-LR	3	0.24
MPI-M	MPI-ESM-MR	3	0.21
MPI-M	MPI-ESM-P	2	0.21
MRI	MRI-ESM1	1	0.28
NASA-GISS	GISS-E2-H	8	0.13
NASA-GISS	GISS-E2-H-CC	1	0.16
NASA-GISS	GISS-E2-R	20	0.13
NASA-GISS	GISS-E2-R-CC	1	0.11
NCAR	CCSM4	8	0.12
NCC	NorESM1-M	3	0.10
NCC	NorESM1-ME	1	0.10
NOAA-GFDL	GFDL-ESM2G	1	0.20
NOAA-GFDL	GFDL-ESM2M	1	0.19
NSF-DOE-NCAR	CESM1-BGC	1	0.12
NSF-DOE-NCAR	CESM1-CAM5	3	0.17
NSF-DOE-NCAR	CESM1-FASTCHEM	3	0.12
NSF-DOE-NCAR	CESM1-WACCM	1	0.13
Ensemble Mean			**0.14**

References in Supplementary Information

Andreu-Hayles, L., Planells, O., Guti??rrez, E., Muntan, E., Helle, G., Anchukaitis, K.J., Schleser, G.H., 2011. Long tree-ring chronologies reveal 20th century increases in water-use efficiency but no enhancement of tree growth at five Iberian pine forests. Glob. Chang. Biol. 17, 2095–2112. doi:10.1111/j.1365-2486.2010.02373.x

Arneth, a, Arneth, a, Lloyd, J., Lloyd, J., Bird, M., Bird, M., Grigoryev, S., Grigoryev, S., Kalaschnikov, N., Kalaschnikov, N., Gleixner, G., Gleixner, G., Schulze, D., Schulze, D., 2002. Response of central Siberian Scots pine to soil water deficit and long-term trends in atmospheric CO 2 concentration 16.

Berninger, F., Sonninen, E., Aalto, T., Lloyd, J., 2000. Modeling 13C Discrimination in Tree Rings 14, 213–223.

Bert, D., Leavitt, S.., Dupouey, J.L., 1997. Abies Alba During the Last Century. Ecology 78, 1588–1596.

Duquesnay, A, Breda, N., Stievenard, M., Dupouey, J.L., 1998. Changes of tree-ring delta C-13 and water-use efficiency of beech (Fagus sylvatica L.) in north-eastern France during the past century. Plant Cell Environ. 21, 565–572. doi:10.1046/j.1365-3040.1998.00304.x

Feng, X., 1999. Trends in intrinsic water-use efficiency of natural trees for the past 100-200 years: A response to atmospheric CO2 concentration. Geochim. Cosmochim. Acta 63, 1891–1903. doi:10.1016/S0016-7037(99)00088-5

Hemming, D.L., Switsur, V.R., Waterhouse, J.S., Heaton, T.H.E., Carter, a H.C., 1998. Climate variation and the stable carbon isotope composition of tree ring cellulose: an intercomparison of \emph{Quercus robur}, \emph{Fagus sylvatica} and \emph{Pinus silvestris}. Tellus Ser. B-Chemical Phys. Meteorol. 50, 25–33. doi:10.1034/j.1600-0889.1998.00002.x

Katul, G., Manzoni, S., Palmroth, S., Oren, R., 2010. A stomatal optimization theory to describe the effects of atmospheric CO2 on leaf photosynthesis and transpiration. Ann. Bot. 105, 431–442. doi:10.1093/aob/mcp292

Linares, J.C., Delgado-Huertas, A., Camarero, J.J., Merino, J., Carreira, J.A., 2009. Competition and drought limit the response of water-use efficiency to rising atmospheric carbon dioxide in the Mediterranean fir Abies pinsapo. Oecologia 161, 611–624. doi:10.1007/s00442-009-1409-7

Medlyn, B.E., Duursma, R.A., Eamus, D., Ellsworth, D.S., Prentice, I.C., Barton, C.V.M., Crous, K.Y., De Angelis, P., Freeman, M., Wingate, L., 2011. Reconciling the optimal and empirical approaches to modelling stomatal conductance. Glob. Chang. Biol. 17, 2134–2144. doi:10.1111/j.1365-2486.2010.02375.x

Nock, C.A., Baker, P.J., Wanek, W., Leis, A., Grabner, M., Bunyavejchewin, S., Hietz, P., 2011. Long-term increases in intrinsic water-use efficiency do not lead to increased stem growth in a tropical monsoon forest in western Thailand. Glob. Chang. Biol. 17, 1049–1063. doi:10.1111/j.1365-2486.2010.02222.x

Palmroth, S., Katul, G.G., Maier, C.A., Ward, E., Manzoni, S., Vico, G., 2013. On the complementary relationship between marginal nitrogen and water-use efficiencies among Pinus taeda leaves grown under ambient and CO 2-enriched environments. Ann. Bot. 111, 467–477. doi:10.1093/aob/mcs268

Peñuelas, J., Hunt, J.M., Ogaya, R., Jump, A.S., 2008. Twentieth century changes of tree-ring δ13C at the southern range-edge of Fagus sylvatica: Increasing water-use efficiency does not

avoid the growth decline induced by warming at low altitudes. Glob. Chang. Biol. 14, 1076–1088. doi:10.1111/j.1365-2486.2008.01563.x

Sidorova, O. V., Siegwolf, R.T.W., Saurer, M., Naurzbaev, M.M., Shashkin, A. V., Vaganov, E.A., 2010. Spatial patterns of climatic changes in the Eurasian north reflected in Siberian larch tree-ring parameters and stable isotopes. Glob. Chang. Biol. 16, 1003–1018. doi:10.1111/j.1365-2486.2009.02008.x

Sidorova, O.V., Siegwolf, R.T.W., Saurer, M., Shashkin, A. V., Knorre, A.A., Prokushkin, A.S., Vaganov, E.A., Kirdyanov, A. V., 2009. Do centennial tree-ring and stable isotope trends of Larix gmelinii (Rupr.) Rupr. indicate increasing water shortage in the Siberian north? Oecologia 161, 825–835. doi:10.1007/s00442-009-1411-0

Silva, L.C.R., Anand, M., Leithead, M.D., 2010. Recent widespread tree growth decline despite increasing atmospheric CO2. PLoS One 5. doi:10.1371/journal.pone.0011543